

## The Health Protection Agency Radiation Protection Division Passive Survey Instrument

D T Bartlett, L G Hager and R J Tanner

### ABSTRACT

---

Aircraft crew and frequent flyers are exposed to elevated levels of cosmic radiation of galactic and solar origin and secondary radiation produced in the atmosphere, the aircraft structure and its contents. Following recommendations from the International Commission on Radiological Protection, the European Union (EU) introduced a revised Basic Safety Standards Directive which included exposure to natural sources of ionising radiation, including cosmic radiation, as occupational exposure. The revised Directive has been incorporated into laws and regulations in the EU member states. Where the assessment of the occupational exposure of aircraft crew is necessary, the preferred approach to monitoring is by the recording of staff flying times and calculated route doses. However there is a requirement to validate calculations periodically by measurement.

The Radiation Protection Division of the HPA has developed a passive survey instrument to make these measurements. The instrument consists of a box containing 36 etched track detectors and 30 thermoluminescence dosimeters (TLDs), and 2 electronic personal dosimeters (EPDs) to record the time profile of the radiation field. Two boxes are prepared for each measurement, one as a background control. The measurement approach adopted is to determine separately the non-neutron component and the neutron component, which includes neutron-like dose equivalent contribution by high-energy protons. The 15% determination limit (that is the dose which can be determined with a 15% precision) is 100  $\mu$ Sv for the estimation of total ambient dose equivalent. This means that, in general, several return flights are required to make a measurement of acceptable precision.



---

## **CONTENTS**

---

<b>1</b>	<b>Instrument description</b>	<b>1</b>
<b>2</b>	<b>Approach</b>	<b>2</b>
	2.1 Non-neutron component	2
	2.2 Neutron component	3
	2.3 Neutron fields and calibration procedures	4
<b>3</b>	<b>References</b>	<b>8</b>



## 1 INSTRUMENT DESCRIPTION

The Health Protection Agency Radiation Protection Division, HPA-RPD passive survey instrument consists of a glass reinforced polyester (GRP) box of dimensions 255 x 250 x 125 mm containing a central block of 36 etched track detectors arranged in 6 mutually orthogonal stacks of 6 dosimeters in order to have, in aggregate, a response approximately independent of the direction characteristics of the radiation field, 30 thermoluminescence dosimeters (TLDs), and 2 electronic personal dosimeters (EPDs) to record the time profile of the radiation field. The total mass is 4 kg. One of the larger faces of the box is the lid and top of the box. The top generally faces up during measurements in aircraft, and the normal to this surface defines the reference direction of the instrument for calibration. Two boxes are prepared for each measurement, one as a background control.

The 15% determination limit (that is the dose which can be determined with a 15% precision) is 100  $\mu$ Sv for the estimation of total ambient dose equivalent. However, this still means that, in general, several return flights are required to make a measurement of acceptable precision. This is not necessarily a disadvantage where average route doses are being determined. An important consideration, which applies, to a greater or lesser extent, to all devices used to measure such complex radiation fields, is that some *a priori* information on the radiation field is needed to interpret the instrument response.

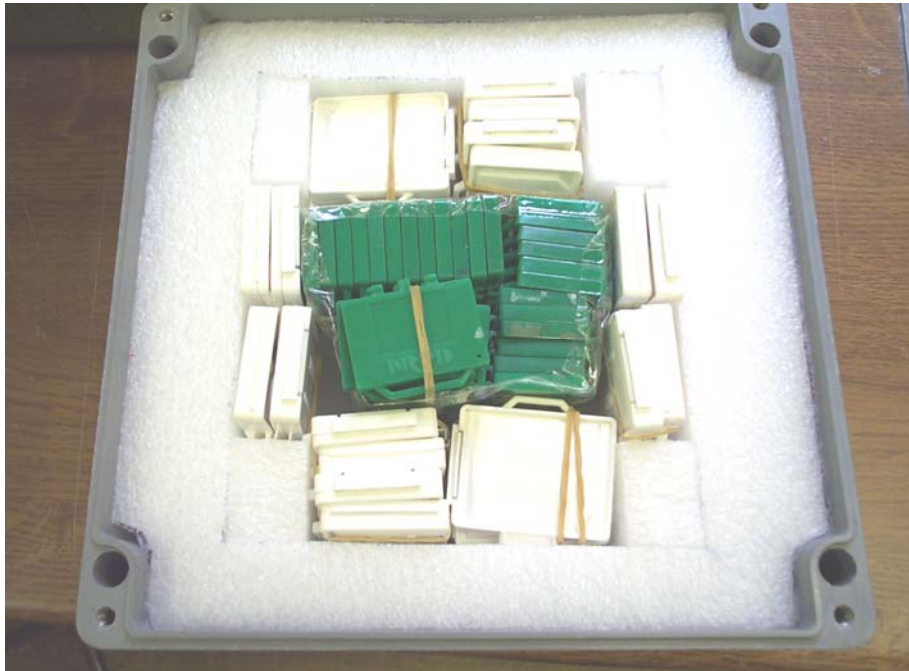


Figure 1 The HPA-RPD passive survey instrument

## 2 APPROACH

---

The cosmic radiation field in aircraft comprises mainly photons, electrons, positrons, muons, protons and neutrons. There is not a significant contribution to dose equivalent from energetic primary heavy charged particles (HZE) or fragments. Details of the composition may be found elsewhere<sup>(1,2,3,4)</sup>. For dosimetric purposes the field can be divided into low and high ( $> 5\text{-}10\text{ keV }\mu\text{m}^{-1}$ ) LET components. The low LET energy deposition can be determined using TLDs. The TLD used should have little response, ideally none, to the high LET component, and an LET-independent absorbed dose response for the low-LET component. With choice of appropriate TL phosphor and suitable calibration, the absorbed dose to tissue can be determined. The high-LET component can be measured using poly allyl diglycol carbonate (PADC, also known by the trade name CR-39<sup>®</sup>) in terms of particle fluence distribution in LET. After the application of the LET/quality factor relationship and with a correction for material composition and density, a determination of tissue dose equivalent can be made to a good approximation<sup>(5)</sup>.

An alternative approach, which is adopted here, is to determine separately two slightly different components, the non-neutron component and the neutron component, which includes neutron-like dose equivalent contribution by high-energy protons. The non-neutron component is determined with TLDs and corresponds to the low-LET component corrected for any neutron contribution. The neutron component plus the nuclear interaction component of the high-energy proton part of the field is determined using PADC detectors with suitable calibration.

### 2.1 Non-neutron component

The non-neutron component comprising photons and directly ionising particles is determined using TLDs. Standard lithium fluoride ( ${}^7\text{LiF:Mg,Ti}$ , 30% loaded PTFE disc) two element dosimeters are used. From an analysis based on photon interaction coefficients calculated by Hubbell<sup>(6)</sup>, tabulations of electron<sup>(7)</sup> and proton<sup>(8)</sup> stopping powers, and data on muon stopping powers<sup>(9,10,11)</sup>, it is concluded that relative to a  ${}^{137}\text{Cs}$  calibration in terms of tissue kerma, the TLDs will give an estimate of absorbed dose to a small mass of tissue for all non-neutron components, to within 5%<sup>(12)</sup>. The energy ranges taken into account include the majority of the contributions to dose<sup>(4,13)</sup>. Further, the results of calculations by Ferrari *et al.*<sup>(14)</sup> would indicate that for the non-neutron component of the field at aircraft altitudes, the depth-dose profile is not pronounced. It is a reasonable approximation, therefore, to apply an ambient dose equivalent calibration of the passive survey Instrument for a  ${}^{137}\text{Cs}$  photon field to the non-neutron or neutron-like field as a whole, with an estimated systematic error of no more than 10%. However the particle type and energy dependence of ambient dose equivalent response for the non-neutron component of the field in aircraft is being investigated further.

In aircraft, the contribution of HZE particles to total ambient dose equivalent is small<sup>(5)</sup>, and the lower light conversion efficiencies of these higher LET particles will reduce their

contribution to the dosimeter reading further. The HZE dose contribution is not considered further.

The  $^7\text{LiF}$  detectors will have some response to the neutron component of the radiation field. Energy deposition from direct nuclear interactions in the detectors and heavy recoils and low energy recoil protons from interactions in the dosimeter holder will be about 1/3 of total neutron kerma, but will have lower relative light conversion efficiency, in the range of 10 to 50% of that to energy deposition for the calibration field. The energy transfer from neutrons to energetic recoil protons will be approximately 2/3 of the total neutron kerma in the material of the passive survey instrument<sup>(15)</sup>, the total kerma factor being similar to that for soft tissue. For energy deposition by the resultant secondary proton energy spectrum, a light conversion efficiency in the range 50 to 100% may be assumed<sup>(16,17)</sup>. The neutron component of the radiation field is about 15% of the total in terms of tissue absorbed dose. Thus the contribution from the neutron (and neutron-like) component to the response of the TLDs is about 5-10%.

The proton fluence and dose distributions in energy at aviation altitudes are peaked around a few hundred MeV<sup>(3,4,18)</sup>, with little dose deposited (at 10 mm depth) by incident protons of energies below 100 MeV or above 10 GeV. Below 100 MeV, protons deposit almost all energy by electromagnetic force (Coulomb) interactions. At higher energies, progressively larger fractions are deposited in a two-stage process with secondary particles being produced by initial strong force interactions, such that at 5 GeV almost all energy deposition by protons is via these neutron-like interactions<sup>(19)</sup>. Integrated over the proton spectrum, about 20% of proton dose, that is 5-6% of the total non-neutron dose component, is deposited by secondary particles from the neutron-like interactions. This analysis is consistent with a mean quality factor for total proton dose of between 1.5 and 2, in agreement with detailed calculations<sup>(20)</sup>. The neutron-like interactions of protons will be registered by the neutron detectors with similar efficiency to neutrons (see below). After taking into account the lower light conversion efficiency of the TLDs for the products of the neutron-like interactions (as in the above consideration of neutron component), a small correction of 2-3% needs to be applied to the response of the TLDs in order to avoid 'double counting' the protons. Taken together, the non-neutron and neutron detectors will, to a reasonable approximation, correctly determine ambient dose equivalent for the proton component. A factor of 0.92 is applied to the ambient dose equivalent ( $^{137}\text{Cs}$  calibration) to account for the contribution to the TLD signal from both neutron and neutron-like energy deposition.

## 2.2 Neutron component

The passive survey instrument uses HPA Personal Dosimetry Services personal neutron dosimeters with PADC detectors which are electrochemically etched and automatically read on a commercial photographic slide scanner with a standard personal computer using customised software<sup>(21,22,23)</sup>. The PADC detectors are used to estimate the neutron plus neutron-like component. Etched track detectors register charged particles by means of etchable damage to the detector structure. The type of material and method of processing (etching) to render the damage observable, determines a threshold rate of energy deposition or material damage along the charged

particle track. This, in turn, determines the types, energies and angles of incidence of charged particles which are detected. Neutrons are detected via secondary charged particles generated in the dosimeter and detector, and also elsewhere in the survey instrument.

The detector responds to particles which deposit energy in the etched volume of the detector with an LET above about  $30 \text{ keV } \mu\text{m}^{-1}$ . This means that, of protons incident on the detector rear surface, only those of energy less than about 800 keV at the surface to be etched are detected by electromagnetic force interactions. Higher energy protons are only detected via other particles generated elsewhere in the instrument as a result of the strong force component of the total interaction cross-section. The proton energy spectrum at each detector will be modified from that incident on the outside of the passive survey meter by slowing down and other interactions. If it is assumed that there is partial radiation equilibrium (the survey meter is about  $6 \text{ g cm}^{-2}$  thick), the proton energy distribution at a detector will be similar to the distribution incident on the box, and will have little fluence below 2 MeV. It is estimated that about 10-20% of the detector reading will be the result of protons' neutron-like behaviour.

The instrument reading integral response characteristic is obtained by folding the monoenergetic response characteristics (see below) with the neutron energy distribution at aircraft altitudes. This is used to convert the values of readings of the PADC detectors obtained for in-flight measurements, to estimate the sum of the neutron component and the nuclear interaction part of the high-energy proton component of ambient dose equivalent for the radiation field being assessed.

### 2.3 Neutron fields and calibration procedures

Measurement of the energy dependence of neutron fluence response of the passive survey instrument has been carried out for the energy range 144 keV to 19 MeV at the Physikalisch-Technische Bundesanstalt (PTB) and in the 60, 68, 96 and 173 MeV quasi-monoenergetic beams at the Université Catholique Louvain (UCL) and The Svedberg Laboratory (TSL), Uppsala University. The results of irradiations at iThemba LABS to quasi-monoenergetic beams of energies 100 and 200 MeV is in progress. All irradiations were carried out to a total fluence corresponding to an ambient dose equivalent in the range 1-3 mSv. The reference point for the instrument was taken to be the centre of the sensitive volume of the PADC detectors.

The neutron irradiation facilities at the PTB national standards laboratory are well characterized. For the irradiations reported here, the scatter component in terms of ambient dose equivalent was less than 1%; and the total uncertainty in the fluence was between 4 and 5%<sup>(24)</sup>. The box was positioned with the front face of the instrument at a distance of 50 cm from the target. The neutron fields provided at UCL, a description of which may be found in the papers by Dupont *et al.*<sup>(25)</sup> and Schuhmacher *et al.*<sup>(26)</sup>, and in [24], are quasi-monoenergetic. The average energy of the peak of the fluence distribution for the neutron beam used was 60.2 MeV, with a width of about 2 MeV. The beam is monitored with a fission chamber and a plastic scintillator. The absolute neutron fluence is determined using a proton recoil telescope. The fraction of neutron fluence

within the peak ( $E_n > 56$  MeV) is 0.32 (fraction of  $H^*(10)$  of 0.26). The fluence energy distribution above 5 MeV has been determined using time-of-flight techniques. Below 5 MeV,  $\Phi_E$  has been assumed constant. The relative uncertainty in the total fluence was determined to be 7%. The box was moved through the beam in such a way as to achieve uniform irradiation. The neutron fields provided at TSL, a description of which may be found in the paper by Condé<sup>(27)</sup>, are also quasi-monoenergetic. The average energies of the peaks of the fluence distributions for the neutron beams used were 68, 96 and 173 MeV, with a width of about 2 MeV. The neutron beam is monitored by means of a thin film breakdown counter (TFBC)<sup>(28,29,30)</sup>. There are some data on the neutron energy distribution above about 30 MeV determined from both measurements and calculations (see Prokofiev<sup>(31)</sup> and references therein). Calculated distributions<sup>(31)</sup> have been used in these investigations for the 68 and 96 MeV neutron beams. The distribution for the 174 MeV beam was extrapolated from published data for a 160 MeV beam<sup>(31)</sup>. Below about 40 MeV, the fluence energy distributions ( $\Phi_E$ ) have been extrapolated to lower energies with  $\Phi_E$  constant. The ratio of peak fluence to total depends on peak energy, but is about 0.4. The uncertainty on the peak fluence was about 10%. The uncertainties in the total fluences are estimated to be 30-35%, when the significant uncertainties in the energy distributions are taken into account. Irradiations were carried out at a distance of 18 m, such that the beam encompassed the entire box.

The results of the measurements are given in Table 1. Both the fluence and ambient dose equivalent dependence of response characteristics are given. The fluence to ambient dose equivalent and effective dose (ISO) conversion coefficients were taken from the International Commission on Radiation Units and Measurements Report 57<sup>(32)</sup> extended to higher energies using values calculated by Ferrari and Pelliccioni<sup>(33)</sup>. In the case of the quasi-monoenergetic fields, the fluence response characteristic for the fluence peak was determined by an iterative fitting method to subtract the instrument reading due to non-peak neutrons. For each TSL neutron field, but starting with the lowest peak neutron energy, a first estimate of the peak energy fluence response characteristic was taken from results for single detector irradiations with monoenergetic protons for energies at, or close to, the peak neutron energies. Together with the results of the lower neutron energy response determinations, a full set of energy response characteristics were constructed and folded with the energy distributions for the non-peak beam component. The instrument reading calculated thus was subtracted from the observed reading to obtain the instrument response for the peak neutron energy. This value was then substituted for the value of the proton response of single detectors and the procedure repeated. Several iterations were carried out to obtain a final value of the peak response which, when included in the response characteristics, gave agreement of calculated and observed instrument readings. The statistical (type A) uncertainties for the instrument readings (made using a number of different sheets of PADC to obtain a representative value) are combined in quadrature with the total standard uncertainties on the neutron fluences to give the standard uncertainties shown.

**Table 1 Energy dependence of response of HPA-RPD passive survey instrument**

Radiation field	Net tracks <sup>(a)</sup> per unit fluence (cm <sup>2</sup> 10 <sup>-6</sup> )	Net tracks per unit effective dose (ISO) (mSv <sup>-1</sup> )	Net tracks per unit ambient dose equivalent (mSv <sup>-1</sup> )
144 keV (PTB)	2.25 (0.38) <sup>(b)</sup>	66 (11) <sup>(b)</sup>	17.7 (3) <sup>(b)</sup>
542 keV (PTB)	14.1 (1.3)	179 (16)	42.0 (3.9)
1.13 MeV (PTB)	29.9 (2)	239 (16)	70.5 (4.7)
2.5 MeV (PTB)	41.3 (2.3)	206 (11)	99.4 (5.5)
5 MeV (PTB)	38.1 (1.7)	140 (6)	94.1 (4.2)
8 MeV (PTB)	34.8 (1.4)	117 (5)	85.1 (3.4)
14.8 MeV (PTB)	48.0 (2.3)	142 (7)	89.5 (4.3)
19 MeV (PTB)	54.7 (8.2)	159 (24)	93.6 (14)
60.2 MeV (UCL)	51 (5.5)	143 (14)	139 (15)
68 MeV (TSL)	42 (13)	115 (36)	121 (37)
95 MeV (TSL)	30 (9)	75 (23)	103 (31)
97 MeV (iThemba)	39 (6)	98 (20)	135 (28)
173 MeV (TSL)	20 (6)	38 (11)	80 (24)

(a) Average for three angles of incidence

(b) Statistical uncertainty (1 s) on instrument reading added in quadrature to total standard uncertainty on fluence.

The fluence energy dependence of response shown is folded with the calculated fluence energy distribution at aircraft altitudes<sup>(2,3)</sup>, to obtain the instrument reading integral response characteristic for aircraft measurements. An estimate of the uncertainty in the integral response characteristic of 13% due to the uncertainty in the measured response characteristics is obtained by folding the values plus or minus one standard deviation. (The sheet to sheet variability is taken into account by using results from the CERF repeatability measurements). Table 2 shows the isotropic field instrument integral response characteristic for the neutron field in aircraft, plus the calculated and measured response characteristics for the CERF energy distribution. For neutron energies below 144 keV for which no response measurements have been made, extrapolation of the response has been made based on the response characteristics for a single PADC detector for isotropic irradiation<sup>(23)</sup>. Given the large uncertainties in the response data there is good agreement. The uncertainty shown is obtained as the half range of calculated integral fluence and ambient dose equivalent response characteristics for the two energy distributions for the  $\pm 1$  s limits of the monoenergetic and quasi-monoenergetic response characteristics. The uncertainty due to the uncertainty in the neutron energy distribution of the field in aircraft is estimated to be 2%, see Table 3.

**Table 2 Comparison of calculated and measured readings of HPA-RPD passive survey instrument**

Neutron field	Reading per unit fluence <sup>(a)</sup> (cm <sup>-2</sup> 10 <sup>-6</sup> )	H*(10) conversion coefficient (pSv cm <sup>-2</sup> )	H*(10) integral response characteristic (mSv <sup>-1</sup> )
Heinrich <i>et al.</i> <sup>(2,3)</sup> 246 g cm <sup>-2</sup>	18.7 (2.1) <sup>(b)</sup>	230	81 (9) <sup>(b)</sup>
Rancati <i>et al.</i> <sup>(36,38,39)</sup> CERF	25.9 (2.9) <sup>(b)</sup>	260	100 (11) <sup>(b)</sup>
CERF measured <sup>(b)</sup>	31.0 (2.9) <sup>(c)</sup>		

(a): For isotropic irradiation (average of three orientations)

(b): Range (approximation to s) for envelope of integral response characteristic  $\pm 1$  s

(c): Standard deviation (s) of repeated measurements mixed photon/neutron radiation fields.

**Table 3 Calculated integral response characteristics of HPA-RPD passive survey instrument in different cosmic radiation field neutron energy distributions.**

Neutron energy distribution	Altitude or atmospheric depth		H*(10)/ $\Phi$ (pSv <sup>-1</sup> )	R <sub><math>\phi</math>new</sub> (cm <sup>2</sup> 10 <sup>-6</sup> )	R <sub>H*(10) old</sub> (mSv <sup>-1</sup> )	R <sub>H*(10) new</sub> (mSv <sup>-1</sup> )
Heinrich <i>et al.</i> , 1999 <sup>(3)</sup>	246 g/cm <sup>2</sup>	Calculated	230	18.7 (2.1) <sup>(a)</sup>	78.6 (11.0) <sup>(a)</sup>	81.4 (9.0) <sup>(a)</sup>
Goldhagen <i>et al.</i> , 2004 <sup>(40)</sup>	56 g/cm <sup>2</sup>	measured	224	18.1 (1.8)	79.0 (9.3)	80.8 (8.0)
Goldhagen <i>et al.</i> , 2004 <sup>(40)</sup>	201 g/cm <sup>2</sup>	measured	218	17.6 (1.8)	79.0 (9.5)	80.7 (8.3)
Wiegel <i>et al.</i> , 2004 <sup>(41)</sup>	FL 350	measured	197	15.6 (2.3)	76.6 (12.8)	79.2 (11.7)
Ferrari <i>et al.</i> , 2001 <sup>(4)</sup>	FL 350	calculated	212	17.4 (1.9)	79.9 (10.2)	82.1 (9.0)
Tommasino <i>et al.</i> 2004 <sup>(42)</sup>	FL 350	measured	342	25.9 (3.8)	75.0 (11.7)	75.8 (11.0)
Clem <i>et al.</i> , 2004 <sup>(43)</sup>	56 g/cm <sup>2</sup>	calculated	235	19.2 (2.1)	79.4 (10.0)	81.7 (8.9)

(a): Half-range for envelope of fluence response  $\pm 1$  s (b):  $E_n > 100$  keV only

Frequent checks on the reproducibility of measurements using different batches and sheets of PADC, have been made with the survey instrument in the simulated cosmic radiation neutron field which has been designed and provided at CERN. The facility has been developed and characterized jointly with the EC for the calibration, characterization and intercomparison of the responses of instrument and dosimeters for the purpose of the determination of the neutron component of the cosmic radiation fields at aircraft altitudes, is known as CERF (CERN-EU high-energy Reference Field facility)<sup>(34,35,36)</sup>. The reference fields are created by beams of high energy protons and pions with momenta of either 120 GeV c<sup>-1</sup> (positive or negative) or 205 GeV c<sup>-1</sup> (positive) incident on a copper target, 0.5 m long. There is massive concrete shielding at the side of the beam at the target positions, and, depending on target position, either iron or concrete shields above. Well-characterized reference fields are located both at the side of the target area and on the roof shields. The radiation field in each calibration position has been calculated by using the Monte Carlo code FLUKA<sup>(36,37,38,39)</sup>. Behind the concrete shields, the neutron radiation field replicates the major components of the neutron component of the cosmic radiation field in aircraft. The CERF neutron field has a wide direction distribution. The PADC batch and sheet variability of the CERF non-isotropic integral response characteristic is shown in Figure 2.

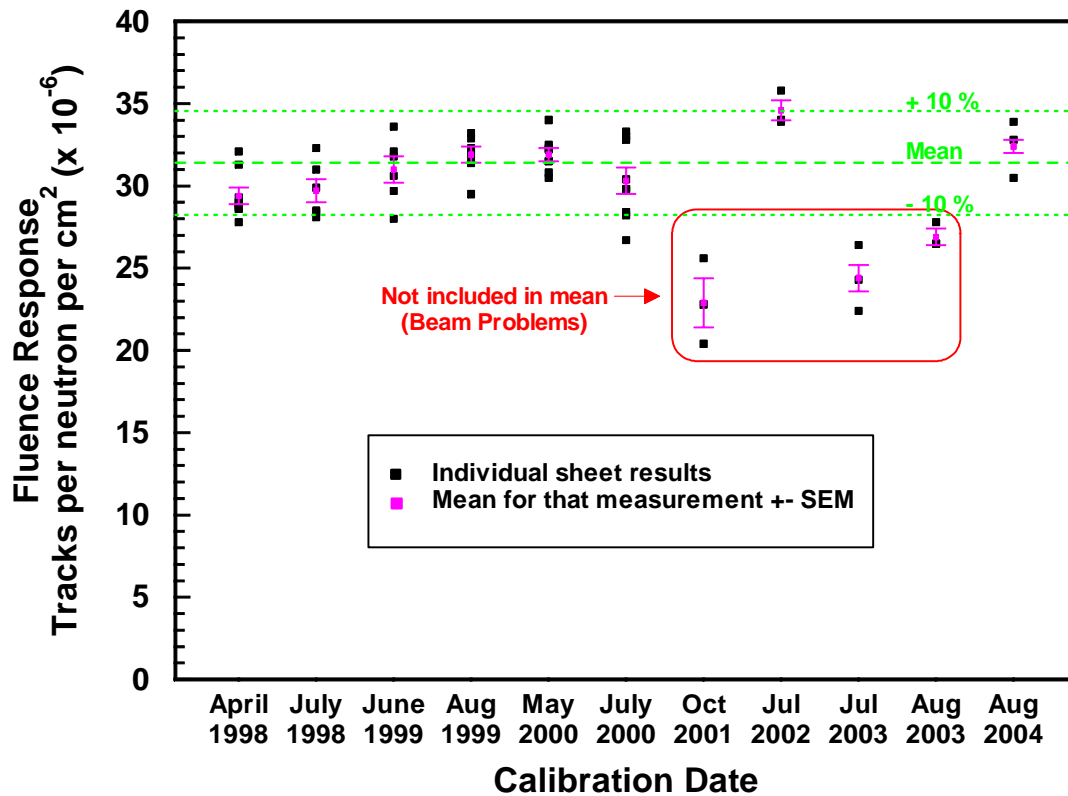


Figure 2 Reproducibility results at CERF

### 3 REFERENCES

- O'Brien, K. The Cosmic Ray Field at Ground Level. Proc. 2nd Int. Conference on Natural Radiation Environment, August 1972, Honiton, USA. Report Conf-720805-PC, 15-54, (US Dept of Commerce: Gaithersburg) (1972).
- Roesler, S, Heinrich, W, and Schraube, H. Calculation of Radiation Fields in the Atmosphere and Comparison to Experimental Data. Radiat. Res. 149 87-97 (1998).
- Heinrich, W, Roesler, S, and Schraube, H. 'Physics of Cosmic Radiation Fields'. Radiat. Prot. Dosim. 86, pp253-258 (1999).
- Ferrari, A., Pelliccioni, M. and Rancati, T. Calculation of the Radiation Environment caused by Galactic Cosmic Rays for Determining Air Crew Exposure. Radiat. Prot. Dosim. 93 101-114 (2001)
- O'Sullivan, D., Zhou, D., Heinrich, W., Roesler, S., Donnelly, J., Keegan, R., Flood, E. and Tommasino, L. Cosmic Rays and Dosimetry at Aviation Altitudes. Radiat. Meas. 31 579-584 (1999).
- Hubbell, J H, and Seltzer, S M. Tables of X-ray Mass Attenuation Coefficients and Mass Energy-Absorption Coefficients, 1 keV to 20 MeV for Elements Z = 1 to 92 and 48 Additional Substances of Dosimetric Interest. National Institute of Standards and Technology Report NISTIR 5632, (US Dept of Commerce: Gaithersburg) (1995).
- International Commission on Radiation Units and Measurements. ICRU Report 37 Stopping Powers for Electrons and Positrons, (ICRU: Bethesda) (1984).

- 8 International Commission on Radiation Units and Measurements. ICRU Report 49 Stopping Powers and Ranges for Protons and Alpha Particles, (ICRU: Bethesda) (1993).
- 9 O'Brien, K. The Response of LiF Thermoluminescence Dosimeters to the Ground-Level Cosmic-Ray Background. *Int. J. Appl. Radiat. Isotop.*, 29, 735–739 (1978).
- 10 Stevenson, G.R. Dose and Dose Equivalent From Muons. European Laboratory for Particle Physics, CERN/TIS-RP/099 (1983).
- 11 Höfert, M. Dosemeter Response to Muons. *Radiat. Prot. Dosim.*, 20, 149–154 (1987).
- 12 Bartlett, D.T., Hager, L.G., Irvine, D. and Bagshaw, M. Measurements on Concorde of the Cosmic Radiation Field at Aviation Altitudes, *Radiat. Prot. Dosim.* 91 365-376 (2000)
- 13 Schraube, H., Leuthold, G., Roesler, S. and Heinrich, W., Experimental and Theoretical Basis of Aviation Route Dose Calculation, *Rad. Res. Congress Proceedings 2* 724-727 (2000).
- 14 Ferrari, A., Pelliccioni, M. and Rancati, T. Study of the Dosimetric Characteristics of Cosmic Radiation at Civil Aviation Altitudes *Radiat. Prot. Dosim.* 102 305-314 (2002)
- 15 Savitskaya, E N, and Sannikov, A V. High Energy Neutron and Proton Kerma Factors for Different Elements. *Radiat. Prot. Dosim.*, 60, 135–146 (1995).
- 16 Jahnert, B. Thermoluminescent Research of Protons and Alpha Particles with LiF (TLD-700). *Proc. 3rd Int. Conf. Luminescence Dosimetry, Risø, 1971. Risø Report 249, pp1031-1039 (Risø: Denmark) (1971).*
- 17 Benton, E.R., Frank, A.L. and Benton, E.V. TLD efficiency of <sup>7</sup>LiF for Doses Deposited by High-LET Particles *Radiat. Meas.* 32 211-214 (2000)
- 18 Ferrari, A, and Pelliccioni, M. Fluence to Dose Equivalent Conversion Data and Effective Quality Factors for Flight Energy Neutrons. *Radiat. Prot. Dosim.*, 76 (4), 215–224 (1998).
- 19 Stevenson, G.R., Private Communication. (1997)
- 20 Pelliccioni, M. Fluence to Dose Equivalent Conversion Data and Radiation Weighting Factors for High Energy Radiation. *Radiat. Prot. Dosim.* 77 (3), 159–170 (1998).
- 21 Bartlett, D T, Steele, J D, Tanner, R J, Gilvin, P J, Shaw, P V, and Lavelle, J. Ten Years On : The NRPB PADC Neutron Personal Monitoring Service. *Radiat. Prot. Dosim.*, 70 (1–4) 161–163 (1997).
- 22 Steele, J D, Bhakta, J R, Bartlett, D T, and Tanner, R J. Development of a Reader for Track Etch Detectors Based on a Commercially Available Slide Scanner. *Radiat. Meas.* 31 179-184(1999).
- 23 Tanner, R.J., Bartlett, D.T. and Hager, L.G. Recent Enhancements to the Understanding of the Response of the NRPB Neutron Personal Dosimeter. *Radiat. Meas.* (2001)
- 24 Alberts, W.G., Arend, E., Barelaud, B., Curzio, G., Decossas, J-L., d'Errico, F., Fiechtner, A., Grillmaier, R., Meulders, J-P., Ménard, S., Roos, H., Schuhmacher, H., Thévenin, J-C., Wernli, Ch. And Wimmer, S. Advanced Methods of Active Neutron Dosimetry for Individual Monitoring and Radiation Field Analysis (ANDO). PTB Report PTB-N-39 (1999).
- 25 Dupont, C., Leleux, P., Lipnik, P., Macq, P. and Ninane, A. Study of a Collimated Fast Neutron Beam. *Nucl. Instrum Meth.* A256 197-206 (1987).
- 26 Schuhmacher, H., Brede, H. J., Dangendorf, V., Kuhfuss, M., Meulders, J.P., Newhauser, W.D. and Nolte, R. Quasi-monoenergetic Neutron Beams with Energies from 25 to 70 MeV. *Nucl. Instrum Meth.* A421 284-295 (1999).
- 27 Condé, H., Hultqvist, S., Olsson, N., Rönqvist, T., Zorro, R., Blomgren, J., Tibell, G., Håkansson, O., Jonsson, O., Lindholm, L., Renberg, P.-U., Brockstedt, A., Ekström, P., Österlund, M., Brady, F.P. and Szefflinski, Z. A Facility for Studies of Neutron-induced Reactions in the 50-200 MeV Range. *Nucl. Instrum. Meth.* A292, 121-128 (1990).
- 28 Tommasino, L., Klein, N. and Solomon, Thin-film Breakdown Counter of Fission Fragments. *P. J. Appl. Phys.* 46 1484-1488 (1975).
- 29 Prokofiev, A.V. and Olsson, N. Fission Fragment Detection Efficiency of Thin-film Breakdown Counters in Sandwich Geometry. Uppsala University Report UU-NF 01#5 (2001).

- 30 Prokofiev, A.V. Smirnov and Renberg, P-U. A Monitor of Intermediate-Energy Neutrons Based on Thin-film Breakdown Counters, Uppsala University Report TSL/ISV-99-0203 (1999).
- 31 Prokofiev, A.V. Nucleon-induced Fission Cross Sections of Heavy Nuclei in the Intermediate Energy Region Ph.D. Thesis Uppsala University (2001)
- 32 International Commission on Radiation Units and Measurements, Conversion Coefficients for Use in Radiological Protection Against External Radiation ICRU Report 57 (ICRU: Bethesda) (1998)
- 33 Ferrari, A. and Pelliccioni, M. Fluence to Dose Equivalent Conversion Data and Effective Quality Factors for High Energy Neutrons. *Radiat. Prot. Dosim.* 76 (4), 215–224 (1998).
- 34 Höfert, M, and Stevenson, G R. The CERN-CEC Reference Field Facility *Proc. Annual Nucl. Soc. 8th Int. Conf. Radiation Shielding.* Arlington, Texas, USA, April 1994, pp635 (1994).
- 35 Stevenson, G R, Fassó, A, Höfert, M, and Tuyn, J W N. Dosimetry at High Energy Accelerators. *Radioprotection* 31 (2), pp193–210 (1996).
- 36 Mitaroff, A. and Silari, M. The CERN-EU High- energy Reference Field (CERF) Facility for Dosimetry at Commercial Flight Altitudes and in Space. *Radiat. Prot. Dosim.* 102 7-22 (2002).
- 37 A. Fassò, A. Ferrari, J. Ranft, P. R. Sala, G. R. Stevenson and J. M. Zazula. FLUKA92. In *Proc. Workshop on Simulating Accelerator Radiation Environment*, Santa Fe, 11–15 January 1993, Ed, Palounek, A, Los Alamos LA-12835-C, 134. (1994)
- 38 Rancati, T, and Ferrari, A. Personal Communication (1996).
- 39 Birattari, C., Rancati, T., Ferrari, A., Höfert, M., Otto, T., and Silari, M. Recent results at the CERN-EC high energy reference facility. In: *Proceedings of the SATIF-3 meeting*, May 12-13, 1997, Sendai, Japan OECD-AENEA, pp219-234, (1998).
- 40 Goldhagen, P., Clem, J.M., and Wilson, J.W. The Energy Spectrum Of Cosmic-Ray Induced Neutrons Measured On An Airplane Over A Wide Range Of Altitude And Latitude, *Radiat. Prot. Dosim.* 110 387-392 (2004).
- 41 Wiegel, B, Wittstock, J, Alevra, A V. And Matzke, M. IN Cosmic Radiation Exposure of Aircraft Crew Compilation of Measured and Calculated Data Final Report of EURADOS WG 5 (European Commission: Luxembourg) (2004).
- 42 Tommasino, L. and Tripathy, S.P. Hardness Ratios of Different Neutron Spectra. *Radiation Protection Dosimetry* 110, 227-231 (2004).
- 43 Clem, J. M., De Angelis, G., Goldhagen, P. and Wilson, J. W. New Calculations of the Atmospheric Radiation Field- Results for Neutron Spectra *Radiat. Prot. Dosim.* 110 423-428 (2004).